2000

Applications of Wavelet Transforms in Biomedical Optoacoustics

Zibiao Wei
Old Dominion University

Shujun Yang
Old Dominion University

Amin N. Dharamsi
Old Dominion University, adharams@odu.edu

Barbara Hargrave
Old Dominion University, bhargrav@odu.edu

Original Publication Citation

Wei, Z., Yang, S., Dharamsi, A. N., & Hargrave, B. (2000). Applications of wavelet transforms in biomedical optoacoustics. *Proceedings of SPIE: BIOS 2000 The International Symposium on Biomedical Optics, 3916,* 249-257. https://doi.org/10.1117/12.386328

Applications of wavelet transforms in biomedical optoacoustics

Zibiao Wei*[a], Shujun Yang[a], Amin Dharamsi[a], Barbara Hargrave[b]

[a]Department of Electrical and Computer Engineering

[b]Department of Biological Science, Old Dominion University, Norfolk, VA 23529

ABSTRACT

We discuss the utility of wavelet transform methods in signal processing in general, and in particular, demonstrate the technique in optoacoustic applications. In several optoacoustic experiments with different samples, we have successfully enhanced the signal to noise ratios. Wavelet transforms optimize resolution by utilizing a tailored, variable time-window in different frequency regions. The technique's great advantage lies in the fact that the wavelet transform adds some redundancy to the original signal, and some desired features can be enhanced in the transformed space. In addition, proper choice of the basis set allows a sparse representation of the signal. Therefore, even when some components are suppressed in the transformed space, the signal itself can maintain its fidelity. This technique has great potential in biomedical optoacoustics, such as medical image processing and signal denoising. We use the wavelet transform technique to resolve acoustic echoes in the time-dilation space (equivalent to the time-frequency space). White noise was removed by the wavelet shrinkage method. This processing was used to analyze several experimental results. These include optoacoustic measurements in solid samples as well as in biological tissues.

Key words: Optoacoustics, biomedicine, wavelet transform, and wavelet shrinkage.

1. INTRODUCTION

Photoacoustics (PA) or optoacoustics (OA) is the generation of acoustic waves by the conversion of incident photons to phonons. The most common mechanism of OA generation is the thermal elastic effect in which the absorbed photons are converted into randomized thermal phonons, followed by length changes in the absorption region. These strains generate stresses that set up propagating acoustic signals. Optoacoustic techniques are used in a variety of applications, including non-intrusive diagnostics of materials. In addition, recent developments allow applications in the biomedical area. While ultrasound imaging has been used for a long time in the medical profession, the availability of pulsed lasers in a large part of the visible and infrared part of the spectrum, has opened the possibility of new applications. Coupled with the fact that there is often a possibility of relatively wide tunability, pulsed lasers have begun to play an important role in advances of optoacoustics in biomedical applications.

In all applications of optoacoustic techniques, including those in the biomedical field, signal processing plays a critical role in the efficacy of the method employed. In this paper, we present results of optoacoustic experiments performed on several materials, including tissues, with an emphasis on the techniques of signal processing. It is shown that a careful analysis of the results, using the new technique of wavelet analysis allows one to extract information about the target from the resulting optoacoustic signals, in a convenient manner. The method allows real-time rapid measurements to be made. When fully developed, the technique would be non-invasive and extremely sensitive. The apparatus is compact, lightweight and inexpensive.

A brief survey of discrete Fourier transform as well as wavelet transform method is given first, followed by a description of the experimental technique. Experimental results are accompanied by signal analyses, and a discussion of the applications is given.

* Correspondence: Email: wei@ece.odu.edu; Telephone: 757 683 4499

In *Biomedical Optoacoustics*, Alexander A. Oraevsky, Editor,
Proceedings of SPIE Vol. 3916 (2000) • 1605-7422/00/$15.00

2. A BRIEF SURVEY OF FOURIER AND WAVELET TRANSFORM TECHNIQUES

The Fourier transform is a well-known and widely used technique. With the advent of digital computers, discrete formulations have gained widespread use. One particularly useful version is the short time Fourier transform (STFT) technique. The idea of STFT is to frame the complete signal into pieces by utilizing a time window. The Fourier transform is applied to each such time window. The STFT is suitable for yielding the time and frequency domain information of a non-stationary signal.

The wavelet transform has two features that often make it more useful than the short time Fourier transform. First, in wavelet analysis, large windows are used to look at gross features, and small windows are used for one to look at finer features. The selection of the window size is performed automatically without the user's intervention. Second, the basis function set used in a wavelet transform can have a variety of forms as long as these basis functions meet certain mathematical requirements. The choice of the basis function is really determined by the data to be represented and the application. If the best wavelets are adapted to the data, or the coefficients are truncated below a threshold, the data can be sparsely represented. This sparse coding makes wavelets an excellent tool in the field of data compression and signal denoising.

Next, the short time Fourier transform is briefly described. Then we introduce the wavelet transform and its varying time-frequency window.

In STFT, a time-localization window $\phi(t-b)$ can be used to segment the signal, and then the Fourier transform of the short time signal is taken. Here, b is the sliding parameter because it determines temporal location of the window. The STFT can be described by:

$$\begin{aligned}(G_\phi f)(b,\xi) &= \int_{-\infty}^{\infty} f(t)e^{-j\xi t}\phi(t-b)\,dt \qquad \text{(time-localization)} \\ &= \frac{e^{-j\xi b}}{2\pi}\int_{-\infty}^{\infty} \hat{f}(\omega)e^{jb\omega}\phi^*(\omega-\xi)\,d\omega \qquad \text{(frequency-localization),}\end{aligned} \tag{1}$$

where f is the signal, b and ξ are used to localize the time and frequency respectively, the carat represents the Fourier transform of the appropriate function, and the star denotes complex conjugation.

It is desired to have a wide time-window to analyze low frequencies thoroughly and a narrow window to locate high frequencies more precisely. Unfortunately, STFT does not have such automatic zoom-in and zoom-out capability. On the other hand, the wavelet transform has this capability.

The wavelet transform can be defined as:

$$(W_\psi f)(b,a) = \frac{1}{\sqrt{a}}\int_{-\infty}^{\infty} f(t)\psi^*\left(\frac{t-b}{a}\right)dt\,, \tag{2}$$

where $\psi(t)$ is the basic wavelet, b is a translation parameter that represents a shift in time, a ($a > 0$) is the dilation parameter representing a frequency shift, $(W_\psi f)(b,a)$ is the wavelet transform coefficient indexed by b and a. The basic wavelet $\psi(t)$ must meet certain conditions, namely $\psi(t)$, $|t|^{1/2}\psi(t)$ and $t\psi(t)$ must be in L^2 and $\hat{\psi}(0) = 0$.

The scale parameter a determines the width of the time and frequency windows. The width of the time window $\frac{1}{\sqrt{a}}\psi(\frac{t-b}{a})$ is $2a\Delta_\psi$, where Δ_ψ the width of the basic wavelet. It can be shown that the width of the frequency window is $\frac{2}{a}\Delta^+_{\hat{\psi}}$, while $\Delta^+_{\hat{\psi}}$ is the width of $\hat{\psi}$, the Fourier transform of the basic wavelet. To map a to an exact frequency, one may consider

$$a \rightarrow \xi = \frac{c}{a}, \text{ for some } c > 0. \tag{3}$$

The constant c is called a calibration constant in frequency units. It is dependent on the wavelet basis, and can be obtained by applying the wavelet transform to a sinusoidal signal with a known frequency.

Now we can see the differences of the STFT and the wavelet transform. While the widths of the time and frequency windows of a STFT transform are rigid, for a wavelet transform the value of a decreases when it locates a wider frequency window and a narrower time window, and vice versa. At the same time, the product of the widths of the time-window and the frequency-window remains constant and obeys the condition

$$\Delta_{\psi}\Delta_{\tilde{\psi}} > \tfrac{1}{2}. \tag{4}$$

Eq. (2) actually defines an integral wavelet transform (IWT) or continuous wavelet transform (CWT). The CWT coefficients can be obtained in a discrete formulation as the following equation:[1]

$$W_{\psi}(b,a) = \left(\frac{\delta t}{a}\right)^{1/2} \sum_{b'=0}^{N-1} x_{b'} \psi^{*}\left[\frac{(b'-b)\delta t}{a}\right], \tag{5}$$

where x is the time sequence with N samples, δt is the sampling period and b and b' are the indexes.

The CWT is often used for applications, such as time-frequency localization, because of its resolution and the redundancy that it introduces. However, the amount of computation is large. To overcome this difficulty, a discrete wavelet transform (DWT) can be used. This is obtained by evaluating the time sequence at the position $b = k/2^{j}$ with binary dilation $a = 2^{-j}$, where j is an integer. It can also be conveniently calculated by utilizing quadrature filters (a pair of complementary low-pass and high-pass filters) and down-sampling technique (up-sampling for the reconstruction).[2] The number of DWT coefficients is the same as the number of the time samplings, but the DWT algorithm is generally much faster.

In most practical applications, the DWT has a large number of coefficients that are zero or small in value if the wavelet basis set is properly chosen. Therefore, a signal can be sparsely represented by it's DWT by ignoring these small or zero coefficients. When necessary, then, the time signal can be reconstructed without any substantial loss in fidelity by padding zeros to the transformed sequence for the purposes of the inverse DWT. This technique has been widely used for data or image compression.

3. APPLICATIONS OF WAVELET TRANSFORM IN BIOMEDICAL OPTOACOUSTIC SIGNAL PROCESSING

3.1. Experimental Arrangement

In our experiment, a pulsed laser beam irradiated the front surface of the sample and a piezoelectric transducer picked up the OA signal at the back. Several samples were used, including materials such as PVC and tissue samples.

The tissue samples were very soft, and a direct contact between the tissue and the transducer results in a distortion of the tissue and the poor reproducibility of the OA experiments. This difficulty can be overcome by using a solid buffer to conduct the OA signal from the tissue to the transducer.

Based on the above considerations, we designed a container to hold the tissue sample (Figure 1). The dimension of the container, which was made out of aluminum, was 1.25"×1.25"×0.4". The tissue sample was immersed in isotonic saline that was in the container. The thickness of the bottom section of the container was about 0.5mm, corresponding to a round trip acoustic delay about 160ns. Although the multi-reflected acoustic signal within the aluminum wall superimposes onto the OA signal (in microsecond scale) generated by the tissue, one is able to observe the main profile of the signal, since the interference is relatively small. The interference can be avoided if the aluminum wall is thick enough; however, this introduces the additional problems, such as acoustic signal attenuation and diffraction.

The samples used in our experiments were muscle tissues taken from a rabbit. The muscle tissue itself appears to be transparent to the eye. However, it has thin connective tissue layers on both surfaces. These connective tissues are white but show differences amongst themselves. For example, one layer, labeled C_1 appears lighter (Figure 1. (a)), while the other visibly distinct layer (Figure 1. (b)), is labeled the C_2 layer.

The OA signals that we observed were generated by these two connective tissues, because they absorbed the pump energy before the light reached the muscle tissue. In our experiments, the C_2 layer generated a larger OA signal than the C_1 layer did.

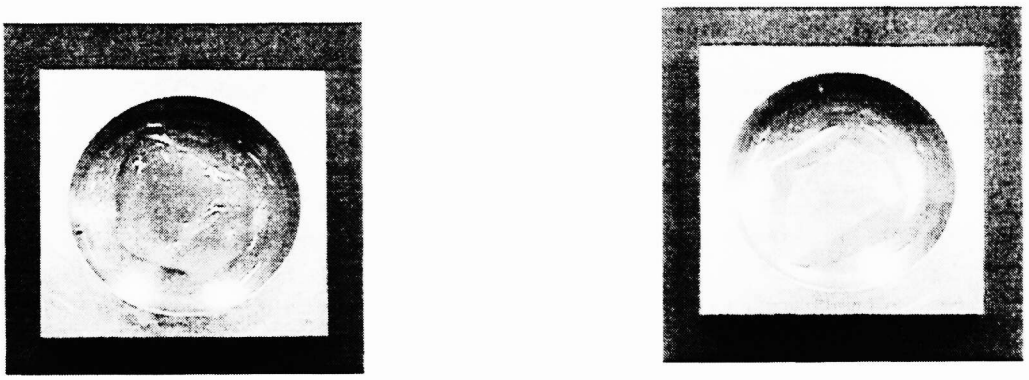

(a) (b)

Figure 1. The aluminum container and the tissue sample: (a) C_1 layer on top. (b) C_2 layer on top.

3.2. Wavelet Transform of OA Signals

One of the sources we used was the passivation light from an excimer laser. The wavelength of the passivation light is 773nm, with a pulsewidth of about 10ns. The energy per pulse was approximately 1mJ. The light pulse was focused onto the tissue sample. Due to the strong scattering property of the tissue and the high energy of the passviation light, some of the incident light was scattered by the sample, reflected by the sidewall of the container and absorbed by the bottom wall. An extra OA signal is hence generated by the aluminum bottom wall. The detected signal is the combination of the OA pulse generated in the tissue, the OA pulse generated in the aluminum wall together with their echoes. These two different types of signals can be identified by the difference of the arrival time. In Figure 2 (a), pulse A is generated by the C_2 connective layer and pulse B is its first echo. Pulse 1 (not displayed in Figure 2 (a)) is the OA pulse generated by the scattered light onto the aluminum bottom. Since it takes a very short time (about 80ns) to arrive at the transducer, this pulse is buried in the RF noise from the discharge of the excimer laser. In this work, we do not use this pulse, since its echoes (pulse 2 and 3) can be clearly seen.

To illustrate that pulse A, B and pulse 2, 3 are generated by different mechanisms, we apply the continuous wavelet transform to the combined signal. In the time-frequency space (Figure 2 (b)), these two types pulses are separated not only in time, but also in frequency. The pulse generated in the aluminum and its echoes have higher frequencies.

3. 3. Signal Denoising By Wavelet Shrinkage

Signal denoising is one of many successful applications of wavelet transform. The principle of denoising by wavelet transform will be described. The improved signal to noise ratio obtained by applying wavelet shrinkage is illustrated below.

Noise exists in all real measurements, and the signal to noise ratio presents a limit to the precision of any measurement. In our OA experiment where a repeatable pulsed laser is used, a convenient and highly effective way to minimize the effects of the random noise is to take multiple measurements and obtain an average from all the acquired signals. However, this method is slow, especially when the laser operates at a low repetition rate. Therefore, it is often not suitable for real-time applications. We show that the wavelet shrinkage method can be used very effectively in such situations.

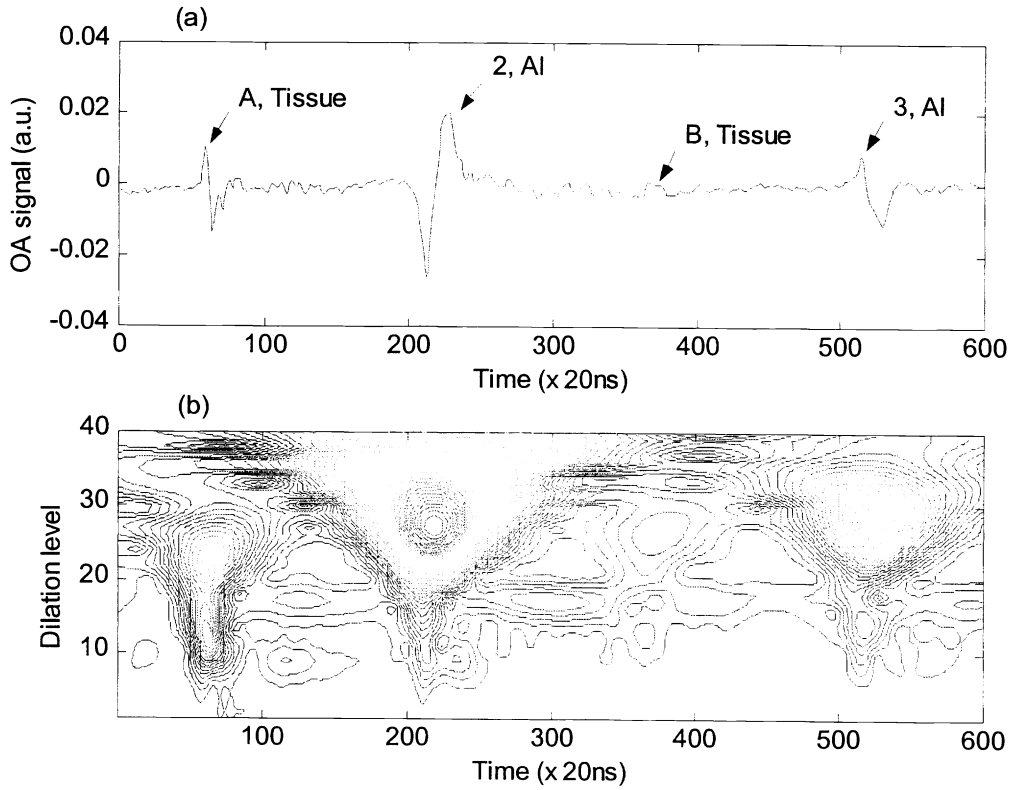

Figure 2. The OA signal obtained with the tissue sample and its continuous wavelet transform: (a) the OA signal that is a combination of pulses generated by the tissue and the aluminum container and their echoes; (b) the continuous wavelet transform of the above signal. A dilation level L corresponds to a dilation parameter $b=2^{L/4}$. The dilation axis is equivalent to the frequency axis but in the opposite direction. Hence a small L represents a high frequency.

The process of removing noise by applying a threshold to the wavelet transform coefficients has been summarized by Donoho, who named this method wavelet shrinkage.[3] Assume that the noisy signal y has n samples, i.e., $y_i = f(t_i) + \sigma z_i, i = 1,...,n$; here $f(t_i)$ is the signal and z_i is a white noise with standard deviation σ. First, one obtains the wavelet coefficients of the noisy data (the noisy signal are preconditioned and normalized to $\sqrt{n}$). Then one applies thresholding to the noisy wavelet coefficients. All coefficients whose absolute values are less than the threshold $t = \sqrt{2\log(n)}\sigma / \sqrt{n}$ are set to zero.

There are two ways to deal with the coefficients whose absolute values are larger than or equal to the threshold t. For *soft-thresholding*, the threshold t is subtracted from each absolute value; while for *hard-thresholding*, these coefficients keep their original values. Finally, one reconstructs the signal using the inverse wavelet transform with the shrunk wavelet coefficients, producing the estimated (less noisy or noiseless) $\tilde{f}(t)$. In the process, forward and inverse discrete wavelet transforms are used for the purpose of simple and fast computation.

For most practical useful signals, only a few discrete wavelet transform coefficients are significant while the rest coefficients are zero or insignificant, since almost all the signals have limited bandwidth. White noise spreads out over all DWT coefficients with small amplitude. This is because the noise has a limited energy content but a wide band spectrum. Therefore, the DWT of a contaminated signal shows several coefficients standing out from the rest of the small coefficients. By setting all insignificant coefficients to zero the wavelet shrinkage can effectively suppress the noise and still keep the signal's fidelity.

3.3.1. An experiment to illustrate the efficacy of denoising.

An experiment utilizing a pulsed nitrogen laser irradiating a PVC sample is discussed, in order to illustrate the method of wavelet shrinkage described above.

The wavelength of the nitrogen laser is 337nm, and the pulsewidth of the laser is about 10ns. The energy per pulse is about $50\mu J$. The laser pulse was incident on the front side of the PVC sample, and the detector was attached to the back of the sample. As expected, the signal is a series of echoes, together with RF noise from the gaseous discharge driving electronics of the Nitrogen laser. A large fraction of the random noise in the signal from a single shot can be effectively removed by a digital scope operating at average mode (at level 256). The averaged signal is used as a reference to be compared with the result from wavelet shrinkage denoising.

Figure 3 shows the denoising process by the wavelet shrinkage method. The noisy signal is plotted in Figure 3(a). It contains 512 samples. The DWT of the noisy signal is plotted in Figure 3(d). The DWT also contains 512 coefficients. Note that in this plot, the vertical axis is the amplitude of the coefficients, and all coefficients are combined and plotted along the horizon axis by both time and frequency in a way described below. The axis is non-uniformly divided into 9 segments. From left to right, each segment contains 2, 2, 4, 8, ..., 256 coefficients. Each segment covers the whole time range, which means that the time sampling rate doubles from one segment to its right neighbor. All coefficients within a segment have the same frequency, and the frequency increases with the power of two segment by segment from left to right.

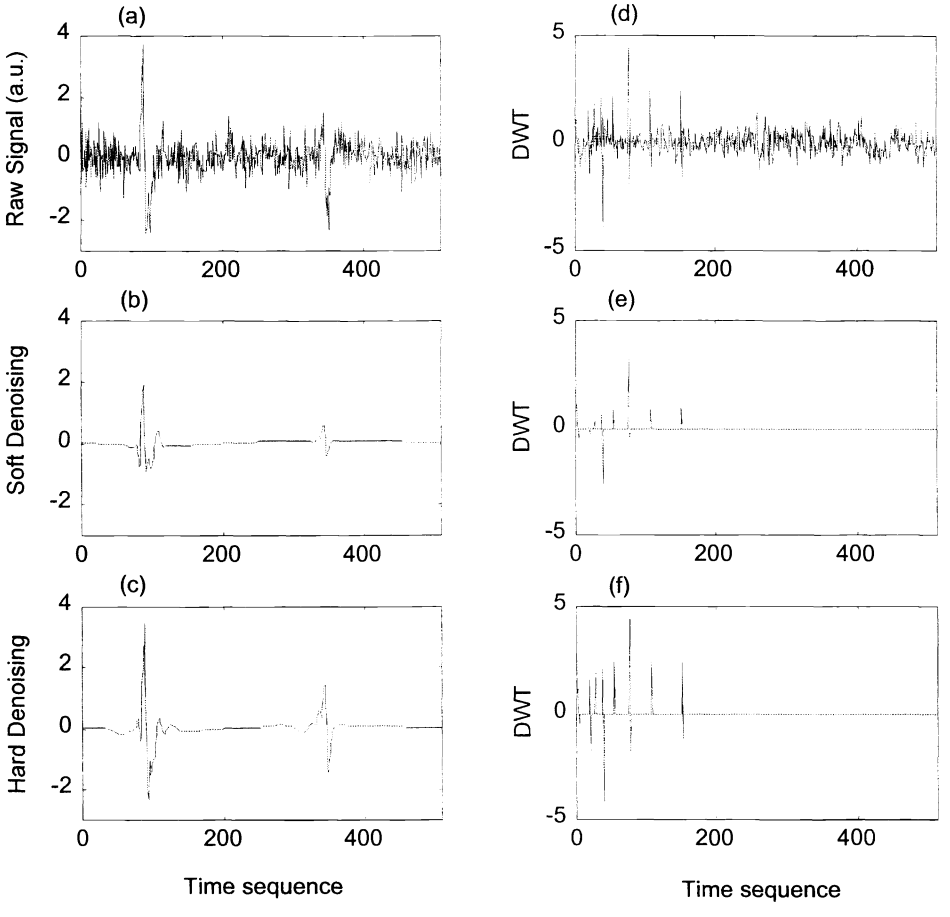

Figure 3. The signal before and after denoising: (a) raw signal; (b) signal denoised by soft thresholding; (c) signal denoised by hard thresholding; (d)-(e) corresponding DWT coefficients to (a)-(c). The threshold for both denoising is set to be 1.5.

In order to use the wavelet shrinkage method, one needs to determine the threshold. For most practical signals, the variance is unknown. Therefore, one has to use an empirical threshold often determined by the visual effect of the output signal. Figure 3(d) shows that the DWT of the noisy signal is also noisy, but all significant coefficients appear at the low frequency region. It is quite safe to assume that all nonzero coefficients in the second half region (between indexes 257 and 512, which is the highest frequency region) are due to the noise and thus can be shrunk to zero. This is because for our experiment (and this is true for many other applications), the signal is over sampled over the Shannon sampling limit. Therefore, at least all DWT coefficients in this region should be zero. For the best visual effect, the threshold can be set to the maximum magnitude of the noisy coefficients in the second half region. In Figure 3, the threshold has been set to 1.5 for both soft and hard thresholding. Both results are visually noiseless. However, if the threshold is set too high, some useful information may also be removed from the signal and errors will be introduced in the result. To reduce the risk of losing useful information, the wavelet basis set that most resemble to the main feature of the time signal needs to be used to perform the DWT. By using the optimized wavelet, the signal can be transformed into less number of DWT coefficients but with higher amplitudes. For this treatment shown in Figure 3, the Coilet-3 wavelet basis was used.

The three results, namely the averaged signal, the one obtained by soft-thresholding and the one by hard-thresholding are superimposed in one plot Figure 4. From this figure, we draw the following conclusions. First, both thresholding methods are able to effectively remove noise and keep the fidelity of the signal, especially in that the signal pulses are not broadened. Second, the result from hard-thresholding maintains the signal amplitude while that from soft-thresholding decreases a little bit in the amplitude. Third, there is a slight distortion of the results from the wavelet shrinkage methods (by the threshold t =1.5). Therefore, as expected there is a tradeoff between removing noise and preserving fidelity of the signal.

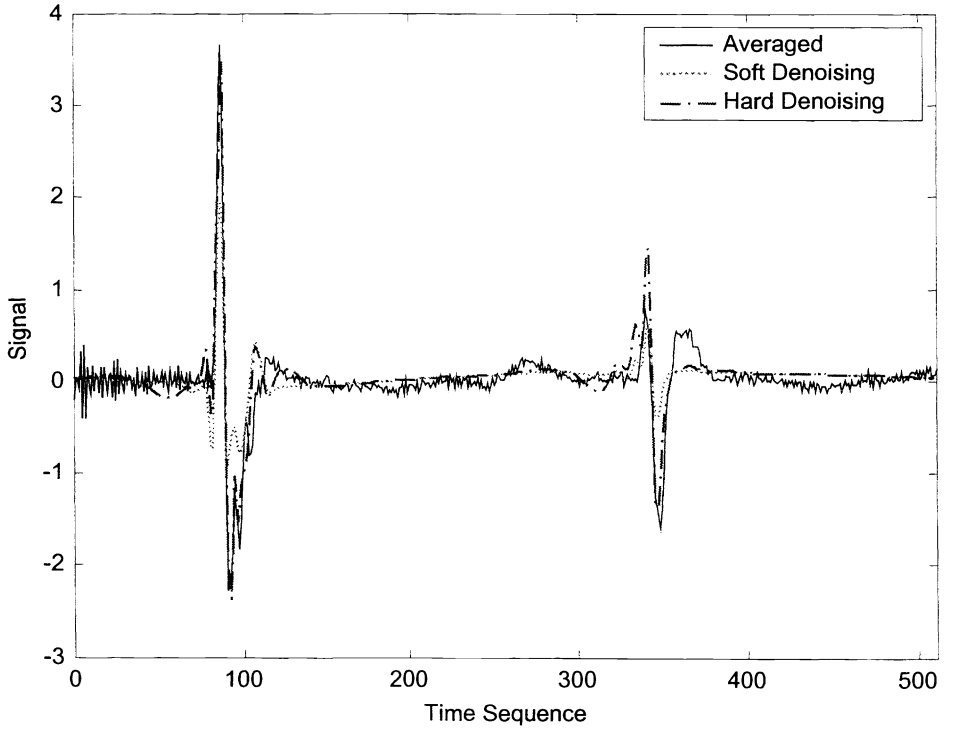

Figure 4. Superimposing the denoising results by three methods: averaging, wavelet soft denoising and wavelet hard denoising.

There are two conventional ways for denoising signals. The first method is the linear smoothing. It slides a window along the time axis. The average of all samples within this window is used as an estimate for the signal at the center of the window. If the time window is too narrow, it cannot remove too many noises. If the window is too wide, it leads to the distortion of the signal. The second method is denoising by filtering. It cannot remove noise within the passband of the used filter. The linear smoothing and the filtering methods can only partially remove the noises. They have difficulties to remove the noise whose

frequency contents fall into the real signal spectrum. The wavelet shrinkage can remove noise while the recovered signal remains its fidelity.

The wavelet shrinkage method is powerful when the noise is white. If the noise is not white, high amplitude wavelet coefficients appear in the transform space. Then the fixed threshold is not reasonable, and a dynamic threshold is effective if the characteristics of the noise are known. There is a tradeoff between removing noise and maintaining fidelity while selecting the threshold for wavelet shrinkage. We have proposed a hybrid method, which combines wavelet shrinkage and the conventional denoising techniques. Our results have showed that this hybrid method has better performance for our applications.

3.3.2. Denoising of signals used in the spectral ratio technique

Wavelet shrinkage is an effective way to denoise OA signals. The process described above has been demonstrated (with the presentation of the results for PVC) to be a useful way to enhance the quality of the data acquired. Here we present some results, obtained by using the same technique, for tissue samples.

We have developed a spectral ratio method for determining the optical absorption coefficient.[4] This technique works best if one is able to eliminate spurious rapid frequency fluctuations. The wavelet shrinkage method, discussed above, is very well suited for such preconditioning of the experimental data used for the spectral ratio technique. The results are presented in this section

An amplitude ratio method has been used to take a measurement of the optical absorption coefficient from OA experimental data by other authors.[5] Their method utilized the amplitude ratio of the OA signal peaks in time domain under the rigid (pressure reflection coefficient $k_r = 1$) and the free boundary ($k_r = -1$) conditions. In this manner, the need for some of the common parameters that are required to describe each signal can be eliminated. The method, however, requires that the experiment be done with the rigid boundary, which cannot be easily fulfilled in many applications. We have proposed a modified spectral ratio method, that takes the advantages of the traditional ratio technique but does not require a rigid boundary to be maintained. Instead, in our modified method, a generally constrained ($-1 < k_r < 1$) boundary condition can be used.

The spectral ratio method takes the ratio of the spectra of two OA signals. If the signals are very noisy, their spectra will also be infected by the noise. Because the ratio operation is nonlinear, some errors, especially in the denominator will be amplified. Here we preconditioned the signals utilizing the wavelet shrinkage method to remove the noise contained in the signals.

Our measurement includes four steps as shown in figure 5. First, we obtained the OA signals under the free and constrained boundary conditions. Next, we used wavelet shrinkage technique to denoise the OA signals. Third, we used the Fourier transform to obtain the spectra of the two signals. Finally, we took the ratio of the two spectra and the used the formula we derived to determine the absorption coefficient. Figure 5 shows the OA signals taken from the C_1 connective tissue excited by the nitrogen laser. The absorption coefficient α, at 337 nm (the wavelength of the nitrogen laser) can be obtained from the slope γ of g versus ω by the following equation:

$$\alpha = \frac{2}{\gamma c_0 (1 + k_r)} \tag{6}$$

where c_0 is the sound velocity in the tissue and k_r is the pressure reflection coefficient at the constrained boundary.

The resultant absorption coefficient of C_1 tissue from Figure 5 is 2.2×10^3 m^{-1}. Similarly, the absorption coefficient of the C_2 tissue at the same wavelength can be obtained and turned out to be 5.8×10^3 m^{-1}. The conclusion that the optical absorption in C_2 tissue is higher than that in the C_1 tissue is consistent with our observation that the OA signal generated by the C_2 tissue is stronger than the C_1 tissue. Also, from the comparison of Figure 5(a) and (b), one sees that the random noise has been effectively removed from the raw signal by the wavelet shrinkage method.

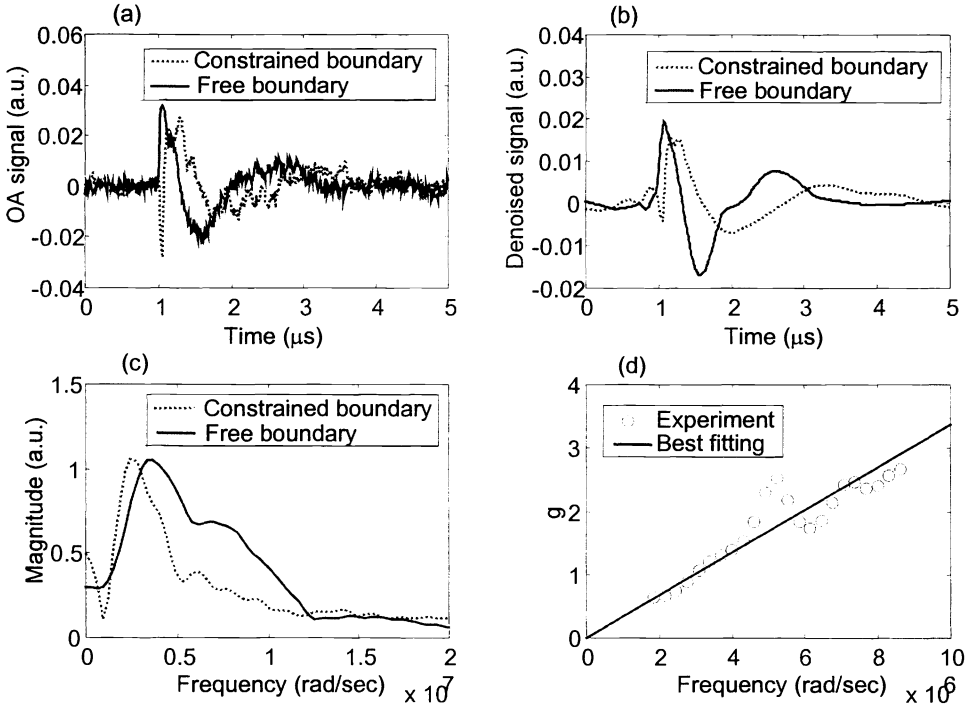

Figure 5. Determining the optical absorption coefficient of the C1 connective tissue at wavelength 337nm: (a) noisy time signals at both boundaries; (b). denoised signals by wavelet shrinkage method; (c) spectra of the denoised signals; (d) best fitting for the parameter g versus frequency, whose slope is used to calculate the absorption coefficient α by Eq. (6). This experiment yields $\alpha(\lambda = 337nm) = 2.2 \times 10^3\ \mathrm{m}^{-1}$.

4. Conclusions

The wavelet transform uses a dynamic time-frequency window to analyze a signal. The resultant transform has high time resolution in the high frequency region as well as high frequency resolution in the low frequency region. The continuous wavelet transform adds redundancy to the signal and provides a powerful tool to interpret the signal in the time-frequency space. We have used the CWT to analyze the optoacoustic signal obtained from a tissue sample. We have successfully identified the OA pulses generated by different media, namely the tissue sample itself and the container that was irradiated by the scattering light from the tissue, from their signatures in the time-frequency space.

The discrete wavelet transform represents a signal sparsely, but accurately. The noise, on the other hand, is not sparsely represented, and this allows one to remove a large fraction of such noise, resulting in dramatic improvements in the signal. We have applied these techniques to several optoacoustic experiments, including those performed on biological tissues. The signal processing technique illustrated in this paper is a powerful tool that can be used in the biomedical imaging. Potential applications involve high spatial resolution of biological samples. In addition, the inherently non-invasive nature of the optoacoustic technique presents researchers with a potential technique that can be used in the real-time medical diagnostic field. The apparatus is compact and relatively inexpensive, and this opens the possibility of widespread use.

REFERENCE

1. C. Torrence, and G. Compo, *Bull. Amer. Meteor. Soc.* **79**, pp. 61,1998
2. M. V. Wickerhauser, *Adapted Wavelet Analysis from Theory to Software*, A K Peters, Wellesley, 1994
3. D. Donoho, *Proceedings of Symposia in Applied Mathematics*, **00**, pp193, 1993
4. Z. Wei, *Ph.D. Dissertation*, Old Dominion University, Norfolk, 2000
5. M. Terzic, and M. W. Sigrist, *J. Appl. Phys.* **67**, pp. 3593, 1990